Synthesis and Characterization of Air-Stable Magnetic Fe Composites Microspheres of Narrow Size Distribution

Nava Shpaisman, Shlomo Margel

Department of Chemistry, Bar-Ilan University, Ramat-Gan 52900, Israel

Received 9 May 2007; accepted 14 August 2007
DOI 10.1002/app.27263
Published online 25 October 2007 in Wiley InterScience (www.interscience.wiley.com).

ABSTRACT: Air-stable Fe magnetic nanoparticles entrapped within carbon and porous crosslinked polystyrene microspheres of narrow size distribution were prepared by the following sequential steps: (1) Polystyrene/poly(divinyl benzene) and polystyrene/poly(styrene-divinyl benzene) uniform micrometer-sized composite particles were prepared by a single-step swelling of uniform polystyrene template microspheres dispersed in an aqueous continuous phase with emulsion droplets of dibutyl phthalate containing the monomers divinyl benzene and styrene and the initiator benzoyl peroxide. The monomers within the swollen polystyrene template microspheres were then polymerized by raising the temperature to 73°C; (2) Porous poly (divinyl benzene) and poly(styrene-divinyl benzene) uniform crosslinked microspheres were prepared by dissolution of the polystyrene template part of the former composite particles; (3) Uniform magnetic poly(divinyl benzene)/Fe and poly(styrene-divinyl benzene)/Fe composite microspheres were prepared by entrapping $Fe(CO)_5$ within the porous crosslinked microspheres, by suction of the Fe complex into the dried porous particles, followed by decomposition of the encapsulated $Fe(CO)_5$ at 200°C in Ar atmosphere; (4) Uniform magnetic air-stable C/Fe composite microspheres were prepared similarly, apart from changing the decomposition temperature from 200 to 600°C. © 2007 Wiley Periodicals, Inc. J Appl Polym Sci 107: 1710–1717, 2008

Key words: air-stable Fe; magnetic microspheres; carbon microspheres

INTRODUCTION

Micrometer-sized particles of narrow size distribution have attracted much attention in many applications such as adsorbents for high-pressure liquid chromatography, calibration standards, spacers for liquid crystals, inks, catalysis, and so forth.[1–7] Dispersion polymerization is the common method for preparing uniform nonporous micrometer-sized particles in a single step.[8–11] However, the particles formed by this method possess a relatively small surface area and their properties, such as porosity, surface morphology and functionality, can hardly be manipulated.[8,11] Furthermore, uniform particles of a diameter larger than 5 μm usually cannot be prepared by dispersion polymerization. These limitations had been overcome by several swelling methods of polystyrene (PS) template micrometer-sized particles with appropriate monomers and initiators, e.g., multi-step swelling,[12–18] dynamic swelling,[19–20] and a single-step swelling,[21] followed by polymerization of the monomers within the swollen template particles.

Of particular interest are micron-sized particles with magnetic properties, which are usually used for separation of the particles and/or their conjugates from undesired compounds via a magnetic field. These particles due to their magnetic properties have several additional biomedical applications, e.g., enzyme immobilization, nucleic acids purification, cell isolation and purification, molecular biology, diagnostics, drug targeting, radio immunoassay, hyperthermia, etc.[22–26] The common micron-sized magnetic particles used for biomedical applications are composed of various iron oxides, e.g., magnetite (Fe_3O_4) and meghemite (γ-Fe_2O_3).[27–30]

Fe particles are of special interest since Fe has a significantly higher magnetic moment than iron oxides. However, Fe particles are easily oxidized, e.g., by air, and thereby significantly lose their main advantage of a very high magnetic moment. This article describes a novel method to synthesize air-stable magnetic micrometer-sized particles of narrow size distribution based on Fe. These particles were prepared by a single-step swelling of uniform PS template microspheres, dispersed in an aqueous continuous phase with emulsion droplets of dibutyl phthalate (DBP) containing the initiator benzoyl

Correspondence to: S. Margel (shlomo.margel@mail.biu.ac.il).

Contract grant sponsors: Minerva Grant (Microscale and Nanoscale Particles and Films), The Israeli Ministry of Commerce and Industry (NFM Consortium on Nanocomposite Particles for Industrial Applications).

peroxide (BP), and the monomer divinyl benzene (DVB), or a mixture of DVB and styrene (S). Uniform PS/PDVB and PS/P(S-DVB) composite particles were then formed by polymerizing the monomers within the swollen PS template microspheres at 73°C. Porous PDVB and P(S-DVB) crosslinked uniform microspheres were prepared by dissolution of the PS template part of the former composite particles. $Fe(CO)_5$ was then entrapped within the porous crosslinked microspheres, by suction of the Fe complex through the dried porous particles. Uniform magnetic PDVB/Fe and P(S-DVB)/Fe composite microspheres were prepared by decomposition of the $Fe(CO)_5$ encapsulated in the former microspheres at 200°C in Ar atmosphere. Uniform magnetic air-stable C/Fe composite microspheres were prepared similarly, apart from changing the decomposition temperature from 200 to 600°C.

EXPERIMENTAL

Chemicals

The following analytical-grade chemicals were purchased from Aldrich (Israel), and were used without further purification: $Fe(CO)_5$ (>99%), BP (98%), DVB (99%), sodium dodecyl sulfate (SDS), polyvinylpyrrolidone (PVP, MW 360,000), ethanol (HPLC), 2-methoxy ethanol (HPLC), dibutyl phthalate (DBP), and methylene chloride (HPLC). Styrene (S, Aldrich 99%) was passed through activated alumina (ICN) to remove inhibitors before use. Water was purified by passing deionized water through Elgastat Spectrum reverse osmosis system (Elga, High Wycombe, UK).

Synthesis of uniform PS template microspheres

PS template microspheres of narrow size distribution were prepared according to the literature.[8–10] In a typical experiment, PS microspheres with an average diameter of 2.3 ± 0.1 μm were formed by introducing into the reaction flask (1-L three-neck round-bottom flask equipped with a condenser and immersed in a constant temperature silicone oil bath at a preset temperature) a solution containing PVP, (3.75 g, 1.5% w/v of total solution) dissolved in a mixture of ethanol (150 mL) and 2-methoxy ethanol (62.5 mL). The temperature of the mechanically stirred solution (200 rpm) was then preset to 73°C. Nitrogen was bubbled through the solution for ca. 15 min to exclude air, and then a blanket of nitrogen was maintained over the solution during the polymerization period. A deaerated solution containing BP (1.5 g, 0.6% w/v of total solution) and S (37.5 mL, 16% w/v of total solution) was then added to the reaction flask. The polymerization reaction continued for 24 h, and was then stopped by cooling to room temperature. The PS microspheres formed were washed by extensive centrifugation cycles with ethanol and then with water. The particles were then dried by lyophilization.

Synthesis of uniform micrometer-sized PS/PDVB and PS/P(S-DVB) composite particles

Uniform micrometer-sized PS/PDVB and PS/P(S-DVB) composite particles were formed by a single-step swelling process, at room temperature, of the PS template particles with DBP (swelling solvent) containing S, DVB, and BP, followed by polymerization at elevated temperature. In a typical experiment, PS template microspheres of 2.3 ± 0.1 μm were swollen up to 7.5 ± 0.7 μm by adding to a 20-mL vial containing 10 mL SDS aqueous solution (0.75% w/v), 1.5 mL methylene DBP containing 10 mg BP and 1.5 mL DVB, or 1.5 mL of a mixture of DVB, and S at a volume ratio DVB/S of 1/1. Emulsion droplets of the swelling solvent were then formed by sonication (Sonics and Materials, model VCX-750, Ti-horn 20 kHz) of the mixture at 48°C for 1 min. An aqueous dispersion (3.5 mL) of the PS template microspheres (7% w/v) was then added to the stirred DBP emulsion. After the swelling was completed and the mixture did not contain any small droplets of the emulsified swelling solvent, as verified by optical microscopy, the diameter of the swollen microspheres was measured. For polymerization of the monomers within the swollen particles, the temperature of the shaken vial containing the swollen particles was raised to 73°C for 24 h. The composite microspheres produced were then washed from undesired reagents by extensive centrifugation cycles with water, ethanol, and again water. The particles were then dried by lyophilization.

Synthesis of uniform crosslinked micrometer-sized PDVB and P(S-DVB) particles

Uniform crosslinked micrometer-sized PDVB and P(S-DVB) particles were prepared by dissolving the PS template part of the PS/PDVB and PS/P(S-DVB) composite particles with methylene chloride:acetone (1 : 2). Briefly, PS/PDVB and PS/P(S-DVB) composite particles, prepared as described in the previous paragraph, were dispersed in 50 mL methylene chloride:acetone (1 : 2), and then shaken at room temperature for ca. 15 min. The dispersed particles were then centrifuged, and the supernatant containing the dissolved PS template polymer was discarded. This procedure was repeated four times with methylene chloride:acetone (1 : 2), ethanol, and water. The crosslinked particles were then dried by vacuum evaporation.

Synthesis of uniform micrometer-sized PDVB/Fe and P(S-DVB)/Fe composite particles

PDVB/Fe and P(S-DVB)/Fe composite particles were prepared by evacuating 500 mg of the dried crosslinked microspheres, prepared as described in the previous paragraph, using a diaphragm vacuum pump for 10 min in a filtration flask closed with a septum, then 4 mL $Fe(CO)_5$ was injected into the filtration flask. The microspheres containing the $Fe(CO)_5$ were then heated to 200°C for 3 h under Ar flow. The formed PDVB/Fe and P(S-DVB)/Fe composite particles were then washed from excess reagents with ethanol using a magnetic bar, and dried by vacuum evaporation.

Synthesis of uniform micrometer-sized C/Fe composite particles

C/Fe composite particles were prepared in a similar way to those of P(S-DVB)/Fe, apart from changing the decomposition temperature from 200 to 600°C.

Characterization of the particles

Optical microscope pictures were obtained with an Olympus microscope, model BX51. Cross-section pictures of the microspheres were characterized with a JEOL JEM-1200EX transmission electron microscope (TEM). Microspheres were embedded in Agar 100, sectioned with an ultratome, and then viewed with the TEM. Dyeing was not necessary for the TEM visualization. High-resolution TEM (HRTEM) images were obtained by employing a JEOL-3010 device with 300 kV accelerating voltage. Samples for TEM and HRTEM were prepared by placing a drop of the diluted sample on a 400-mesh carbon-coated copper grid. Surface morphology was characterized with JEOL scanning electron microscope (SEM), model JSM-840. Particle average size and size distribution of the optical and electronic images were determined by measuring the diameters of more than 100 particles with the image analysis software AnalySIS Auto (Soft Imaging System GmbH, Germany). Elemental analysis of the various particles was performed using an elemental analysis instrument; model EA1110, CE Instruments, Thermoquast. Powder X-ray diffraction (XRD) patterns were recorded using a X-ray diffractometer (model D8 Advance, Bruker AXS) with Cu Kα radiation. Surface area of the various particles was measured by the Brunauer-Emmet-Teller (BET) method, 27 Gemini III model 2375, Micrometrics. Magnetic measurements were performed with PDVB/Fe, P(S-DVB)/Fe, and C/Fe composite particles that were introduced into a plastic capsule. Measurements at room temperature were performed using an Oxford Instrument vibrating sample magnetometer (VSM). Magnetization was measured as a function of the external field being swept up and down ($-14{,}000$ Oe $< H$ applied $< 14{,}000$ Oe, in steps of 200 Oe).

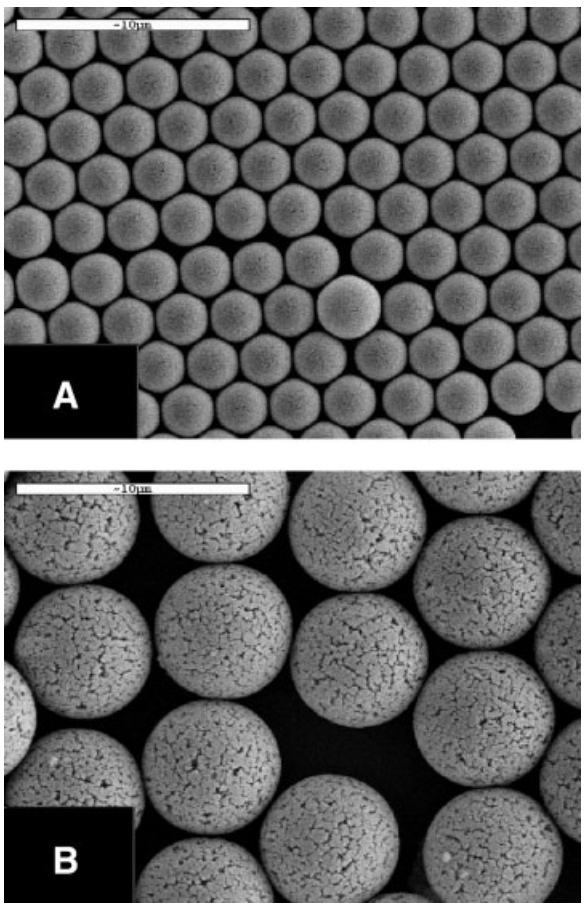

Figure 1 SEM pictures of the PS template microspheres (A) and of the PDVB microspheres (B).

RESULTS AND DISCUSSION

Porous P(S-DVB) and PDVB composite microspheres of narrow size distribution of 6.5 ± 0.2 and 6.3 ± 0.2 μm, respectively, were formed by a single-step swelling process of the uniform PS template microspheres of 2.3 ± 0.1 μm with DBP containing S and/or DVB, followed by polymerization of the monomers within the swollen template microspheres and then dissolving the PS template part.

Figure 1 shows by SEM pictures the spherical shape and narrow size distribution of the PS (A) and of the PDVB (B) microspheres. Figure 1 also illustrates that the surface of the PS template microspheres has smooth nonporous morphology [Fig. 1(A)] while that of the PDVB microspheres is rough and highly porous [Fig. 1(B)]. Similar size and morphology to that of the PDVB microspheres was also demonstrated for the P(S-DVB) composite micro-

spheres. The increased roughness and porosity is expressed by the increased surface area of the PS template microspheres from 2.7 to 222 $m^2\ g^{-1}$ for the P(S-DVB) microspheres, and 530 $m^2\ g^{-1}$ for the PDVB microspheres as measured by BET. The measured surface area of the PS template microspheres is similar to the calculated one ($S = 4\pi r^2$) indicating the nonporous structure of these microspheres. The higher porosity of the P(S-DVB) and PDVB microspheres is due to three main reasons: First, the dissolution of the PS template part of the composite microspheres; second, the swelling solvents serve as porogens that form ''macropores.'' Porogens are substances that are soluble in the monomers, but insoluble in the formed polymers. Thus, pores are formed in the spaces where porogens were extracted from the polymer[31]; Third, the crosslinker monomer DVB leads to the formation of very small pores (''micropores'') as a result of DVB monomeric units tying together linear chains of S at various points,[31] therefore high degree of crosslinker (DVB concentration) increased the surface area.

Magnetic PDVB/Fe and P(S-DVB)/Fe composite microspheres were formed by entrapping $Fe(CO)_5$ within the porous PDVB and P(S-DVB) microspheres, followed by thermal decomposition of the entrapped $Fe(CO)_5$ at 200°C under Ar atmosphere. Figure 2(A,B) represent typical light microscopy pictures of the PDVB and PDVB/Fe composite microspheres, respectively. Figure 2(B) clearly demonstrates the presence of Fe within and on the surface of the composite microspheres. A similar picture was also obtained for the P(S-DVB)/Fe composite microspheres. It should be noted that the yield of these magnetic microspheres was ca. 70%. The other 30% were not attracted to a magnetic bar, and therefore were discarded.

Figure 3 demonstrates cross-sectional typical TEM pictures of a PDVB particle [Fig. 3(A)] and of a PDVB/Fe particle [Fig. 3(B,C); (C) is a higher magnification of (B)]. These pictures clearly demonstrate the presence of Fe nanoparticles of 3- to 30-nm diameter caged in the entire PDVB matrix.

Magnetic air-stable C/Fe composite microspheres were formed by decomposition of the P(S-DVB) microspheres containing $Fe(CO)_5$ at 600°C under Ar atmosphere. Similar trials substituting the P(S-DVB) particles containing $Fe(CO)_5$, for PDVB containing $Fe(CO)_5$, or for PDVB or P(S-DVB) in absence of $Fe(CO)_5$, resulted in the collapse of the microspheres. It seems that for some unclear reason the presence of $Fe(CO)_5$ within the P(S-DVB) microspheres protects the P(S-DVB) microspheres from collapsing during the decomposition at 600°C. The C/Fe formation was executed at 600°C, since at this temperature the Fe nanoparticles entrapped in the carbon microspheres become crystalline.[32]

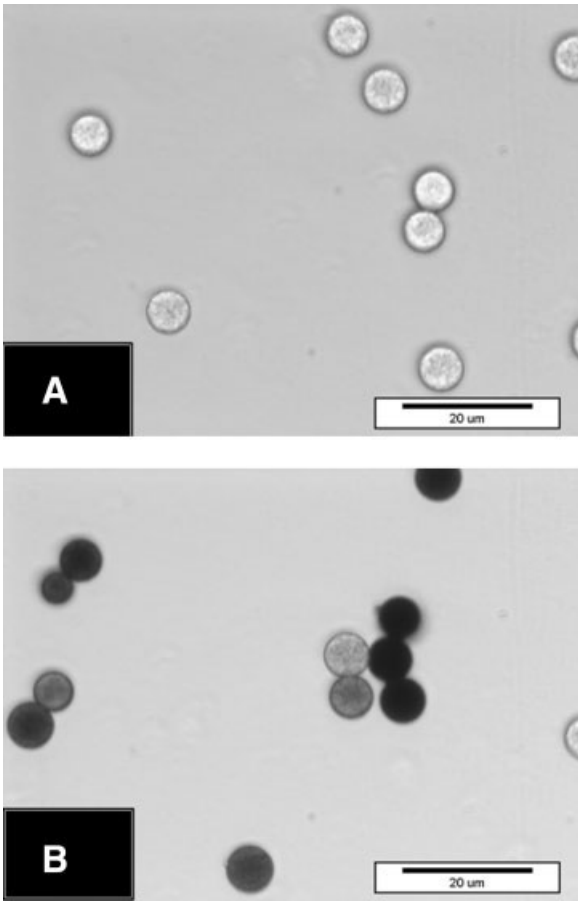

Figure 2 Light microscope pictures of PDVB (A) and PDVB/Fe (B) microspheres.

Figure 4 demonstrates by a SEM picture that the C/Fe composite microspheres possess a spherical shape, bumpy surfaces, and size distribution of 5 ± 0.2 μm. It should also be noted for practical applications, that PDVB, PDVB/Fe, P(S-DVB), P(S-DVB)/Fe, and C/Fe microspheres were all easily dispersed in polar solvents such as water, ethanol, DMF, and methylene chloride.

Table I demonstrates that the Fe content of the PDVB/Fe and P(S-DVB)/Fe composite microspheres increases as the surface area of the parent microspheres, PDVB and P(S-DVB), increases. For example, the Fe content of the PDVB/Fe and P(S-DVB)/Fe is 15.6% and 11.5%, respectively, while the surface area of the microspheres before entrapping the Fe complex is 530 and 222 $m^2\ g^{-1}$, respectively. These results may be explained by the increasing amount of $Fe(CO)_5$ that is entrapped in the pores of the microspheres with larger surface area. It is therefore expected that the surface area of the microspheres containing Fe will be lower than that of the parent microspheres. For example, the surface area of the PDVB and PDVB/Fe microspheres is 530 and 420 $m^2\ g^{-1}$, respectively.

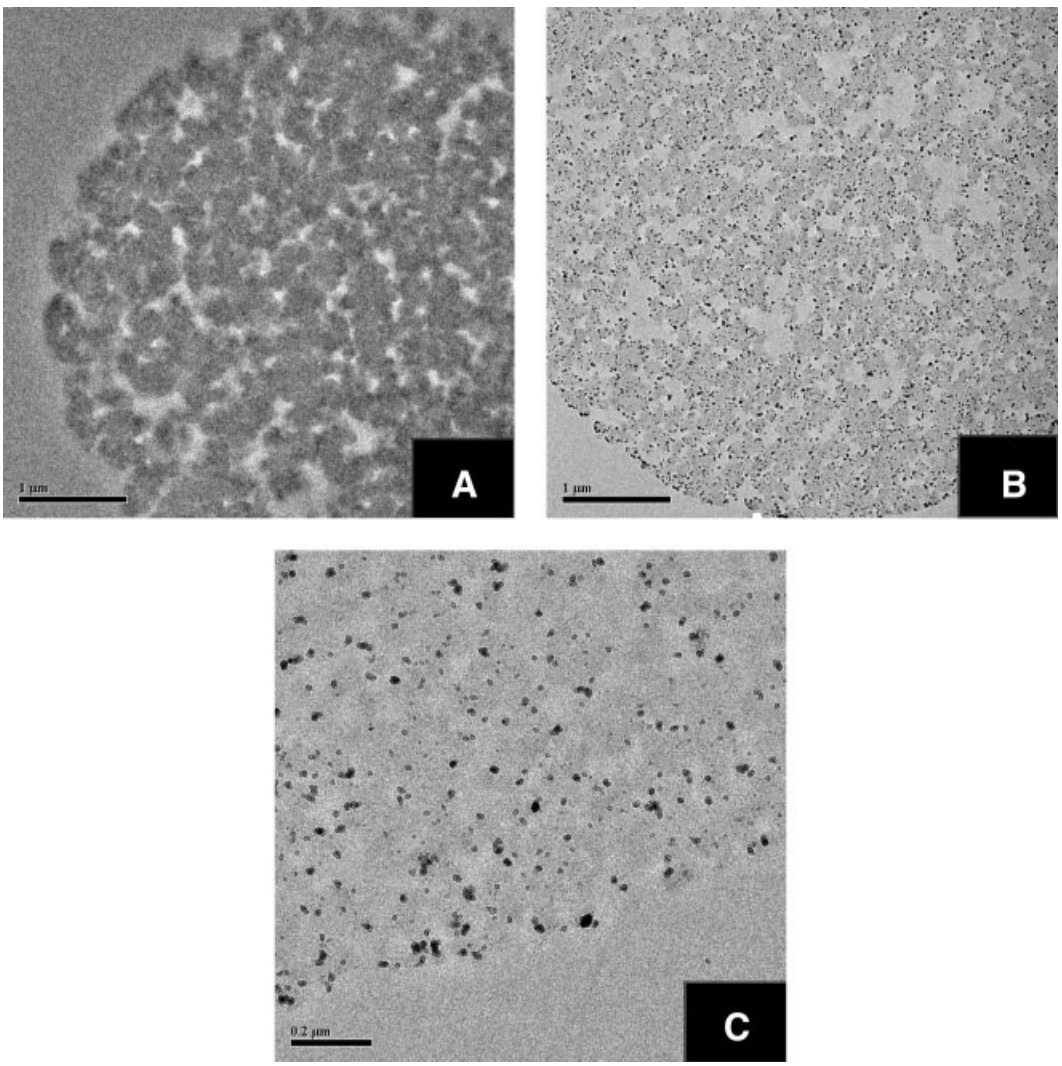

Figure 3 TEM section micrographs of the PDVB (A) and PDVB/Fe composite particles at low (B) and higher (C) magnification.

Table I also illustrates that the C/Fe composite microspheres possess the highest Fe content (33%) and the lowest surface area (38 $m^2\ g^{-1}$). This behavior is probably due to the decomposition of the organic polymeric matrix at 600°C, which increases the weight ratio between the Fe and C and generates relatively closely packed C/Fe particles, as shown in Figure 4.

X-ray powder diffraction analysis was conducted on the PDVB/Fe, P(S-DVB)/Fe, and C/Fe composite microspheres, as shown in Figure 5(A,B), respectively. The PDVP/Fe and P(S-DVB)/Fe composite particles do not display any peaks [Fig. 5(A)], probably due to the high content of the amorphous organic polymer. On the other hand, the C/Fe composite particles exhibit an XRD pattern characteristic of bcc Fe, and a small admixture of Fe_3C and iron oxide [Fig. 5(B)]. The decomposition of the PDVB and P(S-DVB) containing the entrapped $Fe(CO)_5$ at 600°C converted the amorphous organic polymer to a carbon shell containing crystalline Fe nanoparticles. The iron oxide fraction may be located on the microspheres surface.

HRTEM and electron diffraction typical images of the Fe nanoparticles embedded in PDVB/Fe composite microspheres are presented in Figure 6(A,B), respectively. This picture focuses on a Fe nanoparticle belonging to the cross-sectional picture of the PDVB/Fe composite microspheres, shown in Figure 3(C). These measurements were used to probe the composition and crystallinity of the Fe nanoparticles, because in this way it is possible to focus on groups of particles free from interference by the amorphous polymer. Figure 6(A) reveals that the Fe nanoparticles are not single crystals, but perhaps polycrystalline or mixture of crystalline and amorphous material. The *d* spacing measured from the electron diffraction patterns (2.09, 1.45 Å) and the relative

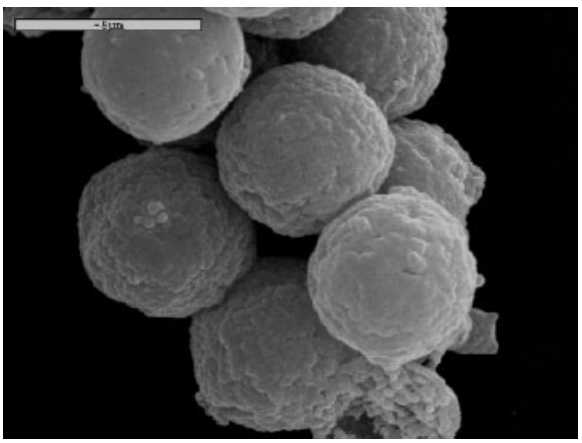

Figure 4 A SEM picture of the C/Fe composite particles.

intensities of the diffraction rings/spots are consistent with bcc Fe (bcc Fe: 2.03, 1.43 Å).[33] The electron diffraction patterns contain a faint ring d = 2.57 Å, which corresponds to Fe_2O_3, which may be due to the oxidation of the Fe nanoparticles on the external part of the PDVB composite microspheres.

Magnetic hysteresis loops of the PDVB/Fe, P(S-DVB)/Fe, and C/Fe composite microspheres are shown in Figure 7. The entire composite microspheres exhibit ferromagnetic behavior and the $M(H)$ plots reach saturation in fields of around 5000 Oe. The coercivity (H_C) of the measured samples is indicated within the plots. M_S values of PDVB/Fe and P(S-DVB)/Fe composite microspheres are 7.6 and 17.7 emu g^{-1}, respectively, (Fig. 7) where the highest values are associated with the samples with the highest Fe loading. The enhancement of the M_S value to 59 emu g^{-1} for the C/Fe composite microspheres is due to its highest Fe loading and to the crystallinity of the Fe nanoparticles. When expressed per gram of iron in the composite microspheres (using Table I), M_S values of the P(S-DVB)/Fe and PDVB/Fe composite microspheres are 66 and 113 emu g^{-1}, respectively, and 179 emu g^{-1} to the C/Fe microspheres, while the reported value of bcc Fe is 222 emu g^{-1}.[34]

The lower saturation magnetization of the PDVB/Fe, P(S-DVB)/Fe, and C/Fe composite microspheres is related to the nature of the nanoparticles, which contain some amorphous Fe (156 emu g^{-1}),[35] iron oxide (75 emu g^{-1}), and Fe_3C (14 emu g^{-1}).[36] The measured coercivity of the PDVB/Fe and P(S-DVB)/Fe composite microspheres is 64 and 72 Oe, respectively, while that of C/Fe composite microspheres exhibits an H_C of 300 Oe. The coercivity of the PDVB/Fe and P(S-DVB)/Fe composite microspheres, we assume, is an average of superparamagnetic particles which have a zero coercivity, ferromagnetic Fe that has a few tens of Oe, and iron oxide that has a few hundred Oe.[37,38] This is not surprising, since the size of Fe nanoparticles is 3–30 nm (Fig. 3) and Fe particles smaller than 14 nm are expected to be superparamagnetic.[39] The higher coercivity of the C/Fe microspheres (300 Oe) is probably related to the Fe_3C, which has H_C value significantly higher than bcc Fe.[34] Furthermore, it is possible that the decomposition at 600°C increased the Fe nanoparticles size, and thereby converted the superparamgnetic Fe nanoparticles to ferromagnetic, which exhibit a coercivity of a few tens of Oe.

The storage stability at room temperature in air of the PDVB/Fe, P(S-DVB)/Fe, and C/Fe composite microspheres was tested by sequential measurements of elemental analysis, XRD, and magnetic susceptibility. These measurements did not indicate any significant changes during 6-month storage. Also, no visible change was observed during this period of time. These composite particles were also stable for at least 1 week upon contact with water. The air-stable Fe nanoparticles in the PDVB/Fe, P(S-DVB)/Fe composite microspheres is located where there is low surface area, while placed with high surface

TABLE I
%Fe and Surface Area of the P(S-DVB)/Fe, PDVB/Fe, and C/Fe Composite Particles

Composite particles	Fe (wt %)	Surface area (m^2 g^{-1})
PDVB/Fe	15.6	420
P(S-DVB)/Fe	11.5	141
C/Fe	33	38

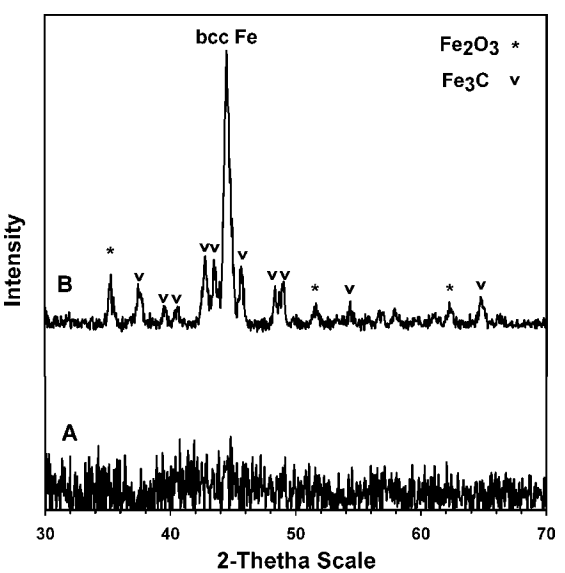

Figure 5 XRD patterns of the PDVB/Fe and P(S-DVB)/Fe composite particles (A) and of the C/Fe (B) composite particles.

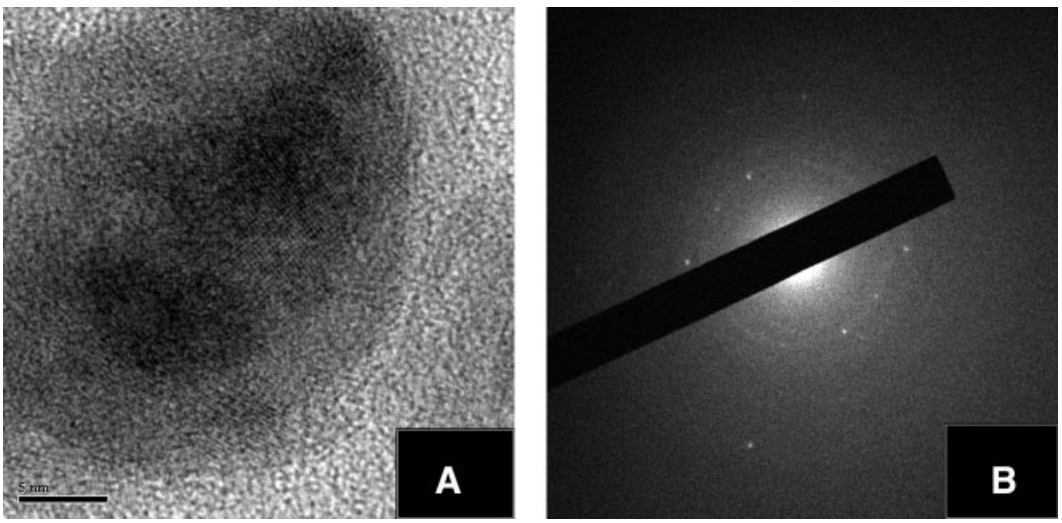

Figure 6 HRTEM pictures (A) and electron diffraction patterns (B) of the Fe nanoparticles embedded in the PDVB/Fe composite particles. This picture presents a higher magnification of the Fe nanoparticles shown in Figure 3(C).

area leads to air oxidation of the Fe to Fe_2O_3. This air oxidation, however, was minimized by the formation of the C/Fe composite microspheres, which exhibit lower surface area and good protection of the carbon coating from Fe oxidation.

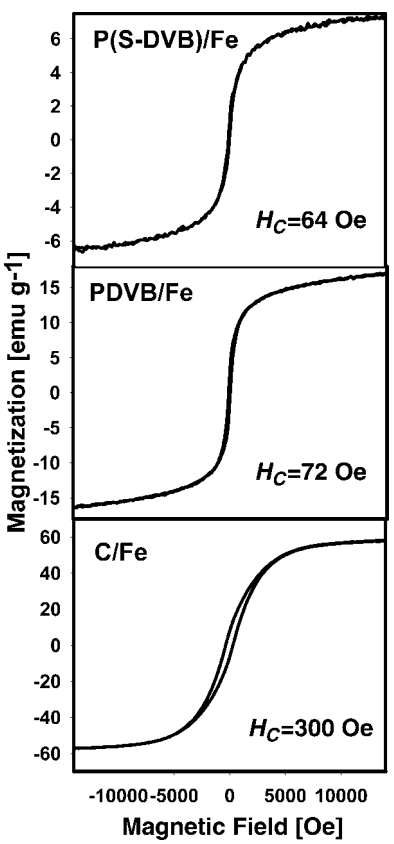

Figure 7 Magnetization curves of the P(S-DVB)/Fe, PDVB/Fe, and C/Fe composite particles.

SUMMARY AND FUTURE PLANS

This article describes a new method for preparation of air-stable magnetic C/Fe, PDVB/Fe, and P(S-DVB)/Fe micrometer-sized microspheres of narrow size distribution. These particles were prepared by entrapping $Fe(CO)_5$ within uniform porous PDVB and P(S-DVB) microspheres. Thermolysis of the $Fe(CO)_5$ entrapped within the former microspheres at 200°C lead to PDVB/Fe and P(S-DVB)/Fe composite microspheres, while thermolysis process at 600°C resulted formation of uniform air-stable magnetic C/Fe composite microspheres. It was interesting to observe that similar thermolysis trials at 600°C substituting the P(S-DVB) microspheres containing $Fe(CO)_5$ for PDVB containing $Fe(CO)_5$, or for PDVB or P(S-DVB) in absence of $Fe(CO)_5$ resulted in the collapse of these microspheres. It seems that for an unclear reason the presence of $Fe(CO)_5$ within the P(S-DVB) microspheres protects the microspheres from collapsing during the decomposition at 600°C. These studies illustrate a direct correlation between the surface area of the PDVB or P(S-DVB) microspheres and their magnetic properties, i.e., the higher the surface area the higher the Fe loading and the saturation magnetization. On the other hand, the high surface area of these composite microspheres leads to air oxidation of surface Fe to Fe_2O_3. This air oxidation, however, was minimized by the formation of the C/Fe composite microspheres, which exhibit lower surface area and good protection of the carbon coating from Fe oxidation. These C/Fe composite microspheres are crystalline and reveal higher saturation magnetization. For future studies we are interested in finding ways to increase significantly the surface area of the C/Fe

composite microspheres, and to use the various magnetic particles described in this manuscript for various biomedical applications, e.g., detoxification, immobilization of bioactive reagents, and cell separation.

We thank Prof. Yossi Yeshurun (Bar-Ilan University, Physics Department, Israel) for his help with the magnetic measurements.

References

1. Arshady, R.; Margel, S.; Pichot, C.; Delair, T. Microspheres, Microcapsules and Liposomes; Citus: London, 1999; Vol. 1, p 165.
2. Margel, S.; Nov, E.; Fisher, I. J Polym Sci Part A: Polym Chem 1991, 29, 347.
3. Margel, S.; Sturchak, S.; Ben-Bassat, E.; Reznikov, A.; Nitzan, B.; Krasniker, R.; Melamed, O.; Sadeh, M.; Gura, S.; Mandel, E.; Michael, E.; Burdygine, I. Microspheres, Microcapsules and Liposomes; Citus: London, 1999; Vol. 2, p 11.
4. Vanderhoff, J. W.; El-Aasser, M. S.; Micale, F. J.; Sudol, E. D.; Tseng, C. M.; Silwanowicz, A.; Sheu, H. R.; Kornfeld, D. M. Polym Mater Sci Eng 1986, 54, 587.
5. Ugelstad, J.; Berge, A.; Ellingsen, T.; Schmid, R.; Nilsen, T. N.; Moerk, P. C.; Stenstad, P.; Hornes, E.; Olsvik, O. Prog Polym Sci 1992, 17, 87.
6. Asua, J. M. Polymeric Dispersions: Principles and Applications; NATO Science Series E: Elizondo, 1997.
7. Margel, S.; Burdygin, I.; Reznikov, V.; Nitzan, B.; Melamed, O.; Kedem, M.; Gura, S.; Mandel, G.; Zuberi, M.; Boguslavsky, L. Recent Res Dev Polym Sci 1997, 1, 51.
8. Bamnolker, H.; Margel, S. J Polym Sci Part A: Polym Chem 1996, 34, 1857.
9. Almog, Y.; Reich, S.; Levy, M. Br Polym J 1982, 14, 131.
10. Paine, A. J. Macromolecules 1990, 23, 3109.
11. Kim, J. W.; Suh, K. D. Polymer 2000, 41, 6181.
12. Ugelstad, J. Makromol Chem 1978, 179, 815.
13. Ugelstad, J.; Moerk, P. C.; Herder Kaggerud, K.; Ellingsen, T.; Berge, A. Adv Colloid Interface Sci 1980, 13, 101.
14. Cheng, C. M.; Micale, F. J.; Vanderhoff, J. W.; El-Aasser, M. S. J Polym Sci Part A: Polym Chem 1992, 30, 235.
15. Hosoya, K.; Frechet, J. M. J. J Polym Sci Part A: Polym Chem 1993, 31, 2129.
16. Smigol, V.; Svec, F.; Hosoya, K.; Wang, Q.; Frechet, J. M. J. Angew Makromol Chem 1992, 195, 151.
17. Smigol, V.; Svec, F. J Appl Polym Sci 1992, 46, 1439.
18. Liang, Y. C.; Svec, F.; Frechet, J. M. J. J Polym Sci Part A: Polym Chem 1997, 35, 2631.
19. Okubo, M.; Ise, E.; Yamashita, T. J Appl Polym Sci 1999, 74, 278.
20. Okubo, M.; Shiozaki, M. Polym Int 1993, 30, 469.
21. Shpaisman, N.; Margel, S. J Chem Mater 2006, 18, 396.
22. Kondo, A.; Fukuda, H. J Ferment Bioeng 1997, 84, 337.
23. Morimoto, Y.; Okumura, M.; Sugibayashi, K.; Kato, Y. J Pharm Dyn 1981, 4, 624.
24. Bushida, K.; Mohri, K.; Katoh, T.; Kobayashi, A. IEEE Trans Magn 1996, 32, 4944.
25. Lin, J. C.; Wang, Y. J. Int J Hyperthermia 1987, 3, 37.
26. Parka, J.; Ima, K.; Leea, S.; Kima, D.; Leea, D.; Leea, Y.; Kimb, K.; Kima, K. J Magn Magn Mater 2005, 293, 328.
27. Ugelstad, J.; Ellingsen, T.; Berge, A.; Helgee, B. W. O. Pat. 8,303,920 (1983).
28. Zhiya, M.; Yueping, G.; Huizhou, L. J Polym Sci Part A: Polym Chem 2005, 43, 3433.
29. Abe, M.; Itoh, T.; Tamaura, Y. Mater Res Soc Symp Proc 1991, 232, 107.
30. Margel, S.; Bamnolker, H. U.S. Pat. 6,103,379 (2000).
31. Sherrington, D. C. Chem Commun 1998, 2275.
32. Shpaisman, N.; Bauminger, E. R.; Margel, S. J Alloys Compd, to appear.
33. Powder Diffraction File; International Centre for Diffraction Data: Swathmore, PA, 1988; File # 6-696.
34. American Society for Metals. Metals Handbook, 9th ed.; American Society for Metals: Metal Park, OH, 1985; Vol. 9: Metallography and Microstructures.
35. Grinstaff, M. W.; Salamon, M. B.; Suslick, K. S. Phys Rev B 1993, 48, 269.
36. Jiao, J.; Seraphi, S.; Wang, X.; Withers, J. J Appl Phys 1996, 80, 103.
37. Tsoukatos, A.; Wan, H.; Hadjipanayis, G. C.; Papaefthymiou, V.; Kostikas, A.; Simopoulos, A. J Appl Phys 1993, 73, 6967.
38. Edelstein, A. S.; Das, B. N.; Holtz, R. L.; Koon, N. C.; Rubinstein, M.; Wolf, S. A.; Kihlstrom, K. E. J Appl Phys 1987, 61, 3320.
39. Cannas, C.; Concas, G.; Gatteschi, D.; Musinu, A.; Piccaluga, G.; Sangregorio, C. J Mater Chem 2002, 12, 3141.